Toward a High-Resolution Structure of Phospholamban: Design of Soluble Transmembrane Domain Mutants†

Sabine Frank,‡,§ Richard A. Kammerer,‡,§ Simon Hellstern,‡ Stefano Pegoraro,|| Jörg Stetefeld,‡ Ariel Lustig,‡ Luis Moroder,|| and Jürgen Engel*,‡

Department of Biophysical Chemistry, Biozentrum, University of Basel, Klingelbergstrasse 70, CH-4056 Basel, Switzerland, and Max-Planck-Institut für Biochemie, D-82152 Martinsried, Germany

Received January 19, 2000; Revised Manuscript Received March 30, 2000

ABSTRACT: Determination of a high-resolution structure of the phospholamban (PLB) transmembrane domain by X-ray crystallography or NMR is handicapped by the hydrophobic nature of the peptide. Interestingly, the crystal structure of the five-stranded parallel coiled-coil oligomerization domain from cartilage oligomeric matrix protein (COMPcc) shows marked similarities to a model proposed for the pentameric transmembrane domain of PLB. Contrary to the putative coiled-coil domain of PLB, COMPcc contains mostly hydrophilic amino acids on the surface, resulting in a soluble molecule. Here, we report the design of soluble PLB transmembrane domain variants by combining the surface residues of COMPcc and the hydrophobic interior of the transmembrane domain of PLB. The soluble PLB variants formed pentameric structures as revealed by analytical ultracentrifugation. After redox shuffling, they showed unspecific disulfide bridge patterns similar to that of the chemically synthesized wild-type PLB transmembrane domain. These results suggest a structural homology between the soluble PLB mutants and the wild-type PLB transmembrane domain. Together with the data reported in the literature, they furthermore indicate that residues Leu37, Ile40, Leu44, and Ile47 of the PLB sequence specify pentamer formation. In contrast, a designed recombinant COMPcc mutant, COMP-ARCC, which was engineered to contain the two PLB cysteines that potentially could form an interchain disulfide bridge, formed a specific disulfide bond pattern. This finding indicates structural differences between the transmembrane domain of PLB and COMPcc. The soluble PLB variants may be used to determine a high-resolution structure of the PLB pentamer by X-ray crystallography.

Phospholamban (PLB)[1] is a 52 amino acid transmembrane protein which regulates the enzymatic activity of the Ca-ATPase in the cardiac sarcoplasmic reticulum (*1*). The protein contains two different domains: a hydrophilic cytosolic domain which contains two phosphorylation sites (residues Ser16 and Thr17) whose phosphorylation relieves the inhibitory effects of the molecule, and a hydrophobic transmembrane domain that is responsible for pentamer formation (*2, 3*). The putative transmembrane domain of PLB is located within residues Gln26−Leu52 and was predicted to form an α-helix sufficiently long to traverse the sarcoplasmic reticulum membrane and when assembled into a pentamer to form a channel structure (*4*−*6*). This domain contains three cysteine residues, Cys36, Cys41, and Cys46, that were proposed to be in reduced form (*4*, *7*). Since structure determination of the transmembrane domain of PLB by X-ray crystallography or NMR has been hindered by the difficulty of investigating such a small, extremely hydrophobic peptide, as yet only models for the α-helical pentamer exist. They have emerged from a combination of spectroscopic techniques (*5*, *8*), molecular modeling (*9*), and mutagenesis studies (*10*−*12*). The model that best satisfied the data is based on formation of leucine−isoleucine zippers between adjacent helices (*12*). It maintains consistency with the structural formalism of coiled coils (*13*) and suggests a left-handed five-stranded parallel coiled-coil conformation for the α-helices with a high level of symmetry. Interestingly, the X-ray structure of the oligomerization domain in cartilage oligomeric matrix protein (COMPcc) shows marked similarities with this model (*14*). COMPcc comprises a five-stranded parallel coiled coil, which is stabilized by a 3,4-hydrophobic repeat. Contrary to the putative coiled-coil domain of PLB, COMPcc contains mostly hydrophilic amino acids on the surface, resulting in a soluble molecule.

Here, we designed two soluble PLB transmembrane domain variants, termed PLB-COMP-1 and PLB-COMP-2, by combining the surface residues of COMPcc and the hydrophobic interior of the transmembrane domain of PLB (Figure 1). The pentameric oligomerization state of the soluble PLB mutants was confirmed by analytical ultracen-

† This work was supported by the Swiss National Science Foundation (Grant 31-49281.96 to J.E.) and by the Bundesamt für Bildung und Wissenschaft (EU program Biotechnology II, EU-No. B104-CT 96.0662 to J.E.).

* Correspondence should be addressed to this author at the Department of Biophysical Chemistry, Biozentrum, University of Basel, Klingelbergstrasse 70, CH-4056 Basel, Switzerland. Phone: +41 61 267−2250. Fax: +41 61 267-2189. E-mail: juergen.engel@unibas.ch.

‡ University of Basel.

§ These authors contributed equally to this study.

|| Max-Planck-Institut für Biochemie.

[1] Abbreviations: COMP, cartilage oligomeric matrix protein; COMPcc, coiled-coil domain of COMP; MBP, maltose-binding protein; PLB, phospholamban; PLB-COMP-1 and PLB-COMP-2, MBP-tagged soluble PLB variants; TSPcc, coiled-coil domain of thrombospondin.

10.1021/bi0000972 CCC: $19.00
Published on Web 05/19/2000

trifugation. The unspecific disulfide bridge patterns (i.e., statistical distribution of disulfide bridges) obtained after redox shuffling by SDS−PAGE analysis suggested a structural homology between the mutants and the PLB transmembrane segment. These results indicate that the substitution of surface residues did not significantly alter the overall structure of the PLB transmembrane domain. Together with the data reported in the literature, these findings suggest that the pentameric structure of the transmembrane domain of PLB is mainly specified by residues Leu37, Ile40, Leu44, and Ile47. As an additional control, we designed COMP-ARCC, a COMPcc mutant that contains cysteines Cys36 and Cys41 of PLB (Figure 1) that potentially could form an interchain disulfide bridge. For this mutant, a specific disulfide bridge pattern (i.e., the highest species observed were pentamers) was obtained, indicating structural differences between COMPcc and the PLB transmembrane domain. Based on these findings, the soluble PLB transmembrane variants should be useful to determine a high-resolution structure of the PLB pentamer by X-ray crystallography.

EXPERIMENTAL PROCEDURES

Construction of Expression Plasmids and Production of Recombinant Proteins. Synthetic genes encoding PLB-COMP-1 and PLB-COMP-2 were prepared by PCR with optimal codon usage for *E. coli* (*15*). The designed mutant polypeptide chain fragment COMP-ARCC was constructed from COMPcc (*16*) by PCR as described by Ho et al. (*17*). The PLB-COMP-1 and PLB-COMP-2 PCR products were ligated into the *Eco*RI/*Pst*I site of the bacterial expression vector pMal-c2 (New England Biolabs). The amplified DNA fragment coding for COMP-ARCC was ligated into the *Bam*HI/*Eco*RI site of the bacterial expression vector pHisTrx2 (*18*). Recombinant insert DNA was verified by Sanger dideoxy DNA sequencing.

The recombinant proteins were expressed in *E. coli* JM109(DE3) host strain (Novagen). Affinity purification of the MBP-tagged fusion proteins PLB-COMP-1 and PLB-COMP-2 was performed under nondenaturing conditions on amylose resin (New England BioLabs) as described in the manufacturer's instructions. Purification of the 6×His-tagged fusion protein COMP-ARCC by immobilized metal affinity chromatography on Ni^{2+}-Sepharose (Novagen) under nondenaturing conditions and separation of the polypeptide chain fragment from the 6×His-tagged carrier protein by thrombin cleavage were carried out as described in the manufacturer's instructions. COMP-ARCC contains two additional residues, Gly and Ser, at its N-terminus. They originate from the expression plasmid and are not part of the COMP coding sequence. The recombinant polypeptide chain fragments were analyzed in 5 mM sodium phosphate buffer (pH 7.4) containing 150 mM NaCl. The concentrations of PLB-COMP-1 and PLB-COMP-2 were determined by tryptophan and tyrosine absorption in 6 M guanidine hydrochloride (*19*), and the concentration of COMP-ARCC was quantitated by the BCA assay (Pierce).

Synthesis of the PLB Transmembrane Domain. Synthesis of the PLBp24-52 peptide comprising residues Ala24−Leu52 was performed in the solid phase using standard Fmoc/tBu chemistry with double coupling and HBTU/HOBt activation (*20*). During synthesis, the cysteine residues were protected as Cys(StBu). The cleavage was performed using trifluoroacetic acid/triisopropylsilane/water (95:1.5:5) to yield the three-Cys(StBu)-protected peptide in good purity. The protected peptide was dissolved in chloroform/trifluoroethanol/water (90:9.5:0.5) and reduced with a 50-fold excess of tributylphosphine for 24 h at room temperature (*21*). The solvent was removed and the peptide precipitated with methyl *tert*-butyl ether, centrifuged, and lyophilized. Mass spectroscopy revealed that more than 90% of the cysteine protecting groups were cleaved (data not shown). The peptide was redissolved in 100 mM Tris-HCl (pH 7.9) supplemented with 4% SDS and dialyzed against 100 mM Tris-HCl (pH 7.9) and 4% SDS for at least 2 days at room temperature.

Gel Electrophoresis. SDS−PAGE and Tricine/SDS−PAGE (*22*) were performed on 12 × 13 cm slab gels. Proteins were visualized by staining with Coomassie Brilliant Blue R-250. Apparent molecular masses were obtained by comparison with low molecular mass markers (Amersham Pharmacia Biotech and Sigma).

Oxidative Disulfide Cross-Linking. Recombinant proteins PLB-COMP-1, PLB-COMP-2, and COMP-ARCC were reduced with 10 mM dithiothreitol for 1 h at 37 °C, precipitated with 75% ammonium sulfate, and redissolved in 200 mM Tris-HCl (pH 8.0), 200 mM NaCl, and 1 mM EDTA. For reoxidation of cysteines, oxidized and reduced glutathione were added to final concentrations of 9 and 0.9 mM, respectively (*16*). After 2 days, the peptides were dialyzed against 5 mM sodium phosphate buffer (pH 7.4) containing 150 mM NaCl.

The chemically synthesized PLB peptide was reduced with 10 mM dithiothreitol for 1 h at 37 °C in 100 mM Tris-HCl (pH 7.9) containing 4% SDS. For redox shuffling of the cysteines, oxidized and reduced glutathione were added to final concentrations of 29 and 0.9 mM, respectively. After 2 days, the peptide was dialyzed against 100 mM Tris-HCl (pH 7.9) containing 4% SDS.

CD Spectroscopy. The CD spectra of COMP-ARCC and PLBp24-52 were acquired on a Jasco J720 spectropolarimeter (Japan Scientific Co.). The far-ultraviolet spectra (200−250 nm) were measured in a 1 mm path length quartz cell and represent averages of 10 accumulations. The spectra were normalized for concentration and path length to obtain the mean molar residue ellipticity after subtraction of the buffer contribution. Helix content was calculated according to Chen et al. (*23*). The temperature scans were recorded on a Cary 61 spectropolarimeter (Varian) equipped with a thermostated 1 mm path length quartz cell. Thermal stability was determined by monitoring the change in the mean molar residue ellipticity at a fixed wavelength of 221 nm, $[\theta]_{221}$, as a function of temperature. A scan rate of 1 °C/min was used. Data analysis was performed with the Jasco (Japan Spectroscopic Co.), LABView (National Instruments), and Sigma Plot (Jandel Scientific) software packages.

Alkylation. PLB-COMP-1 was reduced by incubation with 10 mM dithiothreitol for 1 h at 37 °C and alkylated by addition of 25 mM *N*-ethylmaleimide for 1 h at 37 °C. Subsequently, the peptide was dialyzed against 5 mM sodium phosphate buffer (pH 7.4) containing 150 mM NaCl.

Analytical Ultracentrifugation. Sedimentation equilibrium and sedimentation velocity experiments of disulfide-linked COMP-ARCC and alkylated PLB-COMP-1 were performed

```
databank sequences
                                abcdefg abcdefg abcdefg abcdefg abcdefg abc
rCOMPcc    (27-72):     GDL APQMLRE LQETNAA LQDVREL LRQQVKE ITFLKNT VME CDACG
hCOMPcc    (27-72):     SDL GPQMLRE LQETNAA LQDVRDW LRQQVRE ITFLKNT VME CDACG
hTSP3cc (231-276):      GEQ TKALVTQ LTLFNQI LVELRDD IRDQVKE MSLIRNT IME CQVCG
hPLB       (24-52):          ARQKLQ NLFINFC LILICLL LICIIVM LL

designed mutants
COMP-ARCC          :[GS]GDL APQMLRE LQETNAC LQDVCEL LRQQVKE ITFLKNT VME SDASG
PLB-COMP-1         :           QKLQ NQEINQC LQLICEL LRCIIRM LT
PLB-COMP-2         :           QKLQ NQEINQC LQLICEL LRQIIRM LT
```

FIGURE 1: Design of soluble PLB transmembrane domain variants. Alignment of the amino acid sequences of COMPcc, TSP3cc, the transmembrane domain of PLB, and the designed mutants COMP-ARCC, PLB-COMP-1, and PLB−COMP-2. Heptad positions are indicated by lowercase letters. Numbers refer to amino acid positions within the native proteins. Residues originating from the expression plasmid are shown in parentheses, and cysteine residues are in red. PLB amino acids are indicated in blue, and the COMPcc cysteines that were substituted by serines in COMP-ARCC are in green. r, rat; h, human.

on a Beckman Optima XL-A analytical ultracentrifuge (Beckman Instruments) equipped with 12 mm Epon double-sector cells in an An-60 Ti rotor. The recombinant peptides were analyzed at 20 °C in 5 mM sodium phosphate buffer (pH 7.4) containing 150 mM NaCl. Protein concentrations were adjusted to 0.05−1 mg/mL. Sedimentation velocity runs were performed at a rotor speed of 56 000 rpm, and sedimenting material was assayed by the absorbance at 234 nm. Sedimentation coefficients were corrected to standard conditions (water, 20 °C; *24*). Sedimentation equilibrium scans were carried out at 24 000−32 000 rpm for disulfide-linked COMP-ARCC and at 6800−13 000 rpm for alkylated PLB-COMP-1. Molecular masses were evaluated from ln A versus r^2 plots, where A is the absorbance and r is the distance from the rotor center (*24*). A partial specific volume of 0.73 mL/g was used for all calculations.

RESULTS

Design, Expression, and Characterization of Soluble PLB Mutants. The heptad repeat assignment of the PLB sequence according to Simmerman et al. (*12*) and the sequence alignment of the PLB transmembrane domain, COMPcc, and TSP3cc according to Malashkevich et al. (*14*) are shown in Figure 1. Based on the marked similarities between the PLB transmembrane domain and COMPcc, we engineered a mutant designated PLB-COMP-1 (Figure 1). This peptide was designed to be much more hydrophilic at the surface of the pentamer due to the substitution of eight surface amino acids of the transmembrane domain of PLB by introducing either the corresponding hydrophilic amino acids of COMPcc or the homologous coiled-coil domain of thrombospondin-3 (TSP3cc). Mutagenesis studies of PLB have revealed that individual substitution of these eight amino acids had no significant influence on structure (*11*, *12*). These results are consistent with the assumption that the **b**, **c**, and **f** positions are not essential for maintaining a coiled-coil structure (*25*). Because of these reasons and for the purposes of our study, the **a** and **d** positions are fixed, as are the **e** and **g** residues. It should also be noted that none of the three cysteines of wild-type PLB was replaced in PLB-COMP-1. Because the intrinsic flexibility of the N-terminal cytoplasmic domain (see Discussion) may prevent crystallization of the mutant protein at a later stage in our study, we decided not to include it in our construct. Instead, the recombinant PLB-COMP-1 was fused to the C-terminus of maltose binding protein (MBP) to increase its solubility. The fusion protein was purified as

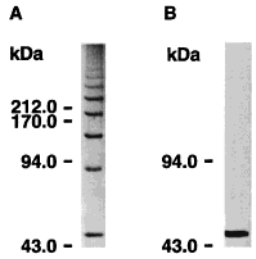

FIGURE 2: Analysis of the recombinant MBP-tagged PLB-COMP-1 polypeptide fragment after redox shuffling. (A) 7% SDS−PAGE under nonreducing conditions. (B) 7% SDS−PAGE under reducing conditions. The migration of marker proteins is indicated.

described under Experimental Procedures. The homogeneity of the recombinant protein was assessed by SDS−PAGE and revealed a single band of the expected monomer molecular mass of 45 kDa for the monomer (Figure 2B).

Following redox shuffling of PLB-COMP-1 with glutathione for 2 days, the unspecific disulfide bridge pattern shown in Figure 2A was obtained by SDS−PAGE. The apparent molecular masses of the species revealed a continuous ladder of molecules, varying by ∼45 kDa. Under reducing conditions, only one single band was obtained (Figure 2B), demonstrating that the disulfide cross-links were formed under nonreducing conditions.

To be able to determine the chain stoichiometry of PLB-COMP-1, the recombinant protein was alkylated prior to analytical ultracentrifugation analysis (Table 1). At 20 °C, 5 mM sodium phosphate buffer (pH 7.4) containing 150 mM NaCl, and protein concentrations below 0.3 mg/mL, sedimentation equilibrium of the PLB-COMP-1 polypeptide chain fragment revealed a molecular mass of 220 kDa. This value corresponds to the molecular mass of a pentamer. At concentrations higher than 0.3 mg/mL, however, the protein started to reversibly associate into higher aggregates. These aggregates probably consist of pentamers which further associated to at least decamers. Their aggregation is most likely due to the hydrophobicity of the PLB-specific amino acids. The molecular masses of the higher aggregates could not be determined due to unideality.

To test whether Cys46 of the PLB peptide is responsible for the unspecific disulfide bond formation, we designed a mutant lacking this residue, termed PLB-COMP-2 (Figure 1). PLB-COMP-2 differs from PLB-COMP-1 by replacement of Cys46 of wild-type PLB by Gln, the corresponding amino acid in COMPcc. After redox shuffling of PLB-COMP-2

Table 1: Sedimentation Coefficients ($s_{20,w}$) and Molecular Masses of MBP-Tagged Alkylated PLB-COMP-1 and Disulfide-Linked COMP-ARCC Polypeptide Chain Fragments[e]

protein	$s_{20,w}$ (S)	molecular mass (kDa) observed	molecular mass (kDa) calculated[a]
PLB-COMP-1	8.0	220[b]	45.0
COMP-ARCC	1.9	12.4,[c] 15.2,[c] 19.9,[c] 25.2[d]	5.2

[a] Molecular mass of the monomer based on its amino acid sequence. [b] The protein was analyzed at six different concentrations ranging from 0.05 to 1 mg/mL at rotor speeds of 6800, 8000, 11 000, and 13 000 rpm. To a concentration of about 0.3 mg/mL, only pentamers are observed. At higher concentrations, the protein reversibly associated into higher aggregates which most likely represent at least decamers. The masses of the higher aggregates could not be determined due to unideality in the measuring cell. [c] Nonhomogeneous molecular mass distributions were observed. The lower number corresponding to the minimum weight near the meniscus is indicated. [d] The protein was analyzed at five concentrations ranging from 0.08 to 0.4 mg/mL at rotor speeds of 24 000, 30 000, and 32 000 rpm. [e] The recombinant polypeptide chain fragments were analyzed at 20 °C in 5 mM sodium phosphate buffer (pH 7.4) containing 150 mM NaCl.

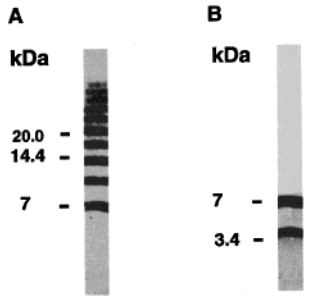

FIGURE 3: Analysis of the chemically synthesized PLB transmembrane domain peptide PLBp24-52 after redox shuffling. (A) Tricine/SDS−PAGE under nonreducing conditions. (B) Tricine/SDS−PAGE under reducing conditions. The migration of marker proteins is indicated.

with glutathione for 2 days, an unspecific disulfide bridge pattern very similar to that of PLB-COMP-1 was obtained (data not shown). This suggests that Cys46 in PLB-COMP-1 does not significantly contribute to the disulfide linkages observed after redox shuffling.

The Cysteine Residues in the PLB Transmembrane Domain Do Not Form Specific Interchain Disulfide Bridges. To test whether the wild-type PLB transmembrane domain forms an unspecific disulfide bridge pattern similar to that of the PLB variants, we chemically synthesized a peptide comprising amino acids Ala24−Leu52 of the human PLB sequence. The PLB transmembrane domain by itself is not soluble except in detergents. Therefore, the CD spectrum from the PLBp24-52 peptide was recorded in 100 mM Tris-HCl (pH 7.9) and 4% SDS. It was characteristic for an α-helical structure with minima near 208 and 222 nm (data not shown). Similar spectra have been reported in previous studies for a PLB transmembrane domain peptide comprising amino acids Gln26−Leu52 (*5*). The temperature-induced unfolding profile recorded at 221 nm revealed no significant loss of helicity in the temperature range of 4−96 °C, indicating high thermal stability of the peptide (data not shown).

After redox shuffling of PLBp24-52 with glutathione for 2 days, SDS−PAGE revealed a continuous ladder of bands (Figure 3A) similar to that of PLB-COMP-1 and PLB-COMP-2. This result is consistent with previous observations

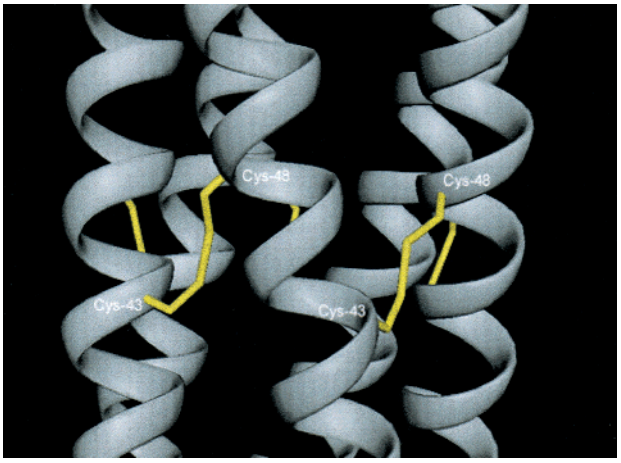

FIGURE 4: Ribbon presentation of a COMPcc-based computer model of COMP-ARCC. The α-helices seen perpendicular to the pentamer axis with their N-termini down are shown in gray. The modeled cysteine residues 43 and 48 at heptad repeat positions **g** and **e**, respectively, are in interchain disulfide bridge distance and are indicated in yellow.

indicating that cysteine residues are in the reduced form (*4*, *7*). The apparent molar mass of the species varied by approximately 3.4 kDa starting with a value of 6.8 kDa. The value of 3.4 kDa is consistent with the calculated molecular mass of the chemically synthesized PLBp24-52 monomer. Under reducing conditions, two bands were observed that correspond to the calculated molecular mass of the monomer and the dimer, respectively (Figure 3B). The inability to obtain only the monomer band of the full-length PLB protein or its transmembrane domain by SDS−PAGE under reducing conditions is in agreement with earlier reports (*6*, *26*, *27*).

Evidence for Structural Differences between the PLB Transmembrane Domain and COMPcc. By assuming a five-stranded coiled coil very similar to that of COMPcc, Cys36 and Cys41 in the transmembrane domain of PLB occupy heptad **e** and **g** positions, respectively (Figure 1). To assay whether in a canonical five-stranded parallel coiled coil an interhelical disulfide bridge pattern similar to those of the wild-type and mutant PLB transmembrane domains is formed, a recombinant COMPcc variant, termed COMP-ARCC, was engineered (Figure 1). COMP-ARCC differs from COMPcc by substitution of Ala43 and Arg48 to cysteines and Cys68 and Cys71 to serines. A COMPcc crystal structure-based computer model indicated that interchain disulfide bridges between the two PLB-derived cysteines in COMP-ARCC are at disulfide bond distance (Figure 4). This particular mutant was produced by heterologous gene expression in *E. coli*. The homogeneity of the affinity-purified recombinant protein was assessed by Tricine/SDS−PAGE (Figure 5B). The protein was soluble, and no degradation products were detected. After redox shuffling of the protein with glutathione for 2 days, specific cysteine-linked species were obtained (Figure 5A). According to their electrophoretic mobilities, they represent a mixture of dimers, trimers, tetramers, and pentamers, with tetramers being the predominant species. In contrast, under the same experimental conditions, the wild-type protein COMPcc predominantly formed pentamers (Figure 5A; see also ref *16*). Under reducing conditions, for both proteins single monomer bands were obtained (Figure 5B), demonstrating that interhelical disulfide bridges were formed under nonreducing conditions.

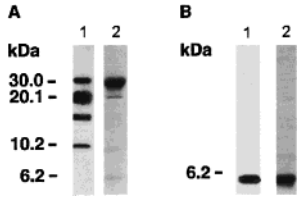

FIGURE 5: Analysis of COMP-ARCC and COMPcc after redox shuffling. (A) Tricine/SDS−PAGE under nonreducing conditions. Lane 1, mutant protein; lane 2, wild-type protein. (B) Tricine/SDS−PAGE under reducing conditions. Lane 1, mutant protein; lane 2, wild-type protein. The migration of marker proteins is indicated.

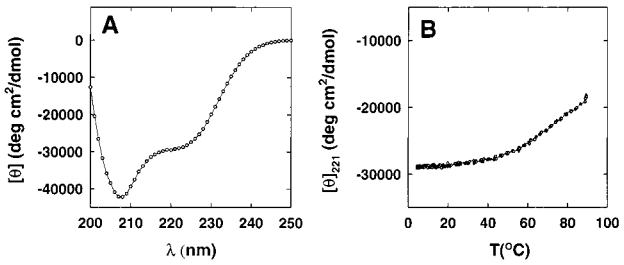

FIGURE 6: CD spectroscopy of the recombinant disulfide-linked COMP-ARCC polypeptide chain fragment. The total chain concentration was 15 μM in 5 mM sodium phosphate buffer (pH 7.4). (A) Far-ultraviolet CD spectrum recorded at 5 °C. (B) Temperature-induced unfolding profile monitored by CD following the change of the mean molar residue ellipticity at 221 nm, $[\theta]_{221}$.

The ability of the COMP-ARCC polypeptide chain fragment to form a coiled-coil structure was verified by CD spectroscopy and analytical ultracentrifugation. At a total chain concentration of 15 μM, disulfide-linked recombinant COMP-ARCC revealed a CD spectrum characteristic for an α-helical structure (Figure 6A). An α-helical content of approximately 85% was predicted from the CD spectrum by assuming that a value of −34 500 deg·cm^2/dmol corresponds to a helicity of 100% for a 47 residue polypeptide chain fragment (*23*). The thermal unfolding profile recorded at 221 nm yielded an approximately 30% decrease of helicity in the temperature range of 4−90 °C (Figure 6B). A similar high thermal stability was also observed for wild-type COMPcc (*28*). As expected for covalently bonded α-helical coiled coils, the melting profile of COMP-ARCC was concentration independent (data not shown).

To determine its chain stoichiometry, the recombinant peptide was analyzed by analytical ultracentrifugation (Table 1). Sedimentation equilibrium measurements of the redox-shuffled COMP-ARCC polypeptide chain fragment at different protein concentrations and rotor speeds yielded molecular masses of 12.4, 15.2, 19.9, and 25.2 kDa, values indicative of a mixture of dimeric, trimeric, tetrameric, and pentameric species (calculated monomer molecular mass of 5.2 kDa). In contrast, the wild-type coiled-coil domain of COMP specifically formed a pentamer at concentrations ranging from 0.2 mg/mL (*29*) to 13 mg/mL (*14*, *16*).

DISCUSSION

The PLB protein contains a single transmembrane helix, which is proposed to form homopentamers that are resistant to gel electrophoresis in 4% SDS. To shed light on the hardly amenable structure of the transmembrane domain of PLB, several, mainly indirect methods were used. The high helical contents of both the full-length PLB and its hydrophobic transmembrane domain were demonstrated by CD in detergents (*5*, *30*) and CD and Fourier transform infrared studies of PLB in lipid bilayers (*8*, *31*). Furthermore, independently two groups performed mutagenesis studies to define the amino acids along the transmembrane domain that are essential for the ability of PLB to form pentamers (*11*, *12*). In one report, a chimeric protein construct, in which *Staphylococcal* nuclease was fused to the N-terminus of PLB, was used for mutagenesis studies of amino acids Phe35−Leu52 of human PLB (*11*). It was investigated, whether the mutants were able to form pentameric complexes similar to the wild-type protein as evidenced by SDS−PAGE. The authors distinguished between disruptive (Leu37, Ile40, Leu44, and Ile47), partially disruptive (Cys36, Leu39, Cys41, Leu43, and Cys46), and nondisruptive (Phe35, Ile38, Leu42, Ile45, Ile48, and Met50) amino acid positions and proposed that nondisruptive positions are oriented outside and disruptive or partially disruptive positions are oriented inside the pentameric structure. The results were consistent with a heptad repeat. A similar approach was made by Simmerman and co-workers (*12*). In their study, the C-terminal amino acids at positions Gln26−Leu52 were mutated separately to Ala or Phe, and the ability of the mutants to form pentameric structures was tested by SDS−PAGE. This experiment revealed that replacement of Leu37, Ile40, Leu44, Ile47, or Leu51 by Ala prevented pentamer formation. The 3,4-residue spacing of these critical amino acids suggests that the sequence from Leu37 to Leu52 adopts a five-stranded coiled-coil structure stabilized by a hydrophobic core consisting of Leu37, Ile40, Leu44, Ile47, and Leu51. These two independently derived sets of mutagenesis data were translated into structural restraints by assuming that sensitive residues are involved in interhelical interactions for generating models of PLB. Two models were proposed, both presenting left-handed symmetrical pentameric coiled-coil structures (*9*, *12*). The models differ by the relative orientation of the five helices by 48 °C, resulting in different interacting residues between helices. The model by Simmerman and co-workers, in which interactions between each pair of subunits are stabilized by a leucine−isoleucine zipper, was further supported by the study of Karim and co-workers (*32*). These authors used results of cysteine reactivity of PLB and its mutants as additional constraints for molecular dynamic calculations.

Despite differences in biological function and lack of sequence identity, marked structural similarities exist between a model of the transmembrane domain of PLB (*12*) and the X-ray structure of the subunit oligomerization domain of COMPcc (*14*). The pentameric structure of COMPcc is achieved through the formation of a parallel α-helical coiled coil that involves 46 N-terminal residues from Gly27 to Gly72. The interchain disulfide bonds between cysteines 68 and 71 further stabilize the five-stranded coiled coil (*16*).

Based on the similarities between the PLB transmembrane domain and COMPcc, we designed two soluble PLB variants by introducing hydrophilic surface residues of COMPcc and TSP3cc. Because the PLB-COMP peptides still tended to aggregate in aqueous solution, we fused them to the C-terminus of the MBP. MBP has been selected because it has been reported that this molecule is uncommonly effective at promoting the solubility of polypeptides to which it is fused (*33*). Furthermore, MBP contains no cysteines, which

was important for our study. As a result, we obtained soluble pentameric PLB variants that tended to associate into higher aggregates as revealed by analytical ultracentrifugation (Table 1).

Importantly, after redox shuffling, similar unspecific disulfide bridge patterns were obtained for the two soluble PLB-COMP mutants (Figure 2A) and the wild-type PLB transmembrane domain (Figure 3A). This suggests their structural homology and together with the data reported in the literature indicates that residues Leu37, Ile40, Leu44, and Ile47 of the PLB transmembrane domain most likely specify the pentamer structure.

To investigate whether the structures of the wild-type and mutant PLB transmembrane domains are similar to that of the five-stranded coiled-coil domain of COMPcc, the mutant COMP-ARCC containing PLB-derived cysteine residues at heptad repeat positions **e** and **g** was designed (Figure 1). Computer modeling predicted that these artificially introduced cysteines are at disulfide bond distance (Figure 4). Indeed, we were able to demonstrate that specific intermolecular disulfide bridges are formed in COMP-ARCC (Figure 5A). However, the mutant COMP-ARCC folded preferentially into tetramers with less dimers, trimers, and pentamers being present, whereas the wild-type COMPcc formed pentameric species under the same conditions (Figure 5A; see also ref *16*). The fact that the high symmetry of the pentamer is influenced by the artificially introduced cysteines in heptad positions **e** and **g** may explain the mixture of oligomerization states which was also found by analytical ultracentrifugation analysis. Consistent with this observation, a switch of the oligomerization state from three- to four-stranded structures has been observed for mutants of residue Gln130 at heptad **e** position in the tenascin-C coiled coil (*18*) and by replacing Arg487 at heptad position **g** in the coiled-coil domain of matrilin 1 (*34*). The effect on the oligomerization state of COMPcc by introducing the two cysteine residues may possibly be also explained in terms of a lower helix propensity of cysteine compared to arginine and alanine (*35*). It is well established that introduction of residues with higher helix propensity can favorably contribute to coiled-coil stability (*35*, *36*). Moreover, it should also be noted that cysteine residues are in general very rare in heptad repeat containing sequences (*37*). Nevertheless, although the oligomeric state was influenced by the introduced cysteines, the ability of COMP-ARCC to form a very stable coiled-coil structure was retained as evidenced by its α-helical CD spectrum and thermal stability. On the basis of these findings, we conclude that structural differences between the PLB transmembrane domain and COMPcc exist.

Recently, Pollesello et al. (*38*) determined the structure of a 36-residue-long N-terminal fragment of phospholamban in aqueous solution containing 30% trifluoroethanol by nuclear magnetic resonance. The peptide, which comprises the cytoplasmic domain and six residues of the transmembrane domain, assumes a conformation characterized by two α-helices connected by a turn. The residues of the turn, Ile19−Pro21, are adjacent to the phosphorylation sites Ser16 and Thr17. Because in the unphosphorylated form determined by Pollesello et al. (*38*) there is no evidence for a constraint position of the N-terminal helices relative to the C-termini, the structure of the cytoplasmic domain fits in any of the structural models proposed for the PLB transmembrane domain. The flexibility of the cytoplasmic domain relative to the transmembrane domain may be important in the kinetics of the monomer to pentamer association, in phosphorylation and dephosphorylation reactions, and in the association of the PLB with the Ca-ATPase in the cardiac sarcoplasmic reticulum.

Taken together, we were able to design soluble PLB variants with structural homology to the PLB transmembrane domain. Because of their increased solubility, these PLB mutants should be more suitable for crystallization than the PLB wild-type domain. Once crystallized, structure determination of the PLB transmembrane domain variants is expected to be straightforward because the high-resolution structure of the MBP component is known. Finally, the atomic structure of the PLB transmembrane domain variants will reveal to which extent the proposed models of the PLB pentamer are correct.

REFERENCES

1. Lindemann, J., Jones, L., Hathaway, D., Henry, B., and Watanabe, A. (1983) *J. Biol. Chem. 258*, 464−471.
2. Wegener, A. D., Simmerman, H. K. B., Liepnieks, J., and Jones, L. R. (1986) *J. Biol. Chem. 261*, 5154−5159.
3. Arkin, I. T., Adams, P. D., Brunger, A. T., Smith, S. O., and Engelman, D. M. (1997) *Annu. Rev. Biophys. Biomol. Struct. 26*, 157−179.
4. Simmerman, H. K. B., Collins, J. H., Theibert, J. L., Wegener, A. D., and Jones, L. R. (1986) *J. Biol. Chem. 261*, 13333−13341.
5. Simmerman, H. K. B., Lovelace, D. E., and Jones, L. R. (1989) *Biochim. Biophys. Acta 997*, 322−329.
6. Tatulian, S. A., Jones, L. R., Reddy, L. G., Stokes, D. L., and Tamm, L. K. (1995) *Biochemistry 34*, 4448−4456.
7. Arkin, I. T., Adams, P. D., Brunger, A. T., Aimoto, S., Engelman, D. M., and Smith, S. O. (1997) *J. Membr. Biol. 155*, 199−206.
8. Arkin, I. T., Rothman, M., Ludlam, C. F., Aimoto, S., Engelman, D. M., Rothschild, K. J., and Smith, S. O. (1995) *J. Mol. Biol. 248*, 824−834.
9. Adams, P. D., Arkin, I. T., Engelman, D. M., and Brunger, A. T. (1995) *Nat. Struct. Biol. 2*, 154−162.
10. Fujii, J., Maruyama, K., Tada, M., and MacLennan, D. H. (1989) *J. Biol. Chem. 264*, 12950−12955.
11. Arkin, I. T., Adams, P. D., MacKenzie, K. R., Lemmon, M. A., Brunger, A. T., and Engelman, D. M. (1994) *EMBO J. 13*, 4757−4764.
12. Simmerman, H. K. B., Kobayashi, Y. M., Autry, J. M., and Jones, L. R. (1996) *J. Biol. Chem. 271*, 5941−5946.
13. Cohen, C., and Parry, D. A. D. (1990) *Proteins: Struct., Funct., Genet. 7*, 1−15.
14. Malashkevich, V. N., Kammerer, R. A., Efimov, V. P., Schulthess, T., and Engel, J. (1996) *Science 274*, 761−765.
15. Dong, H., Nilsson, L., and Kurland, C. G. (1996) *J. Mol. Biol. 260*, 649−663.
16. Efimov, V. P., Engel, J., and Malashkevich, V. N. (1996) *Proteins: Struct., Funct., Genet. 24*, 259−262.
17. Ho, S. N., Hunt, H. D., Horton, R. M., Pullen, J. K., and Pease, L. R. (1989) *Gene 77*, 51−59.
18. Kammerer, R. A., Schulthess, T., Landwehr, R., Lustig, A., Fischer, D., and Engel J. (1998) *J. Biol. Chem. 273*, 10602−10608.
19. Edelhoch, H. (1967) *Biochemistry 6*, 1948−1954.
20. Fields, G. B. (1997) in *Methods in Enzymology: Solid-Phase Peptide Synthesis* (Fields, G. B., Ed.) Vol. 289, pp 3−336, Impressum Academic Press, San Diego, CA.
21. Andreu, D., Albericio, F., Sole, N. A., Munson, M. C., Ferrer, M., and Barany, G. (1994) in *Methods in Molecular Biology* (Pennington, M. W., and Dunn, B. M., Eds.) pp 91−170, Humana Press Inc., Totowa, NJ.

22. Schägger, H., and von Jagow, G. (1987) *Anal. Biochem. 166*, 368−379.
23. Chen, Y.-H., Yang, J. T., and Chau, K. H. (1974) *Biochemistry 13*, 3350−3359.
24. van Holde, K. E. (1985) *Physical Biochemistry*, 2nd ed., pp 93−136, Prentice Hall, Englewood Cliffs, NJ.
25. O'Shea, E. K., Rutkowski, R., and Kim, P. S. (1992) *Cell 68*, 699−708.
26. Jones, L. R., Simmerman, H. K. B., Wilson, W. W., Gurd, F. R., and Wegener, A. D. (1985) *J. Biol. Chem. 260*, 7721−7730.
27. Simmerman, H. K. B., and Jones, L. R. (1998) *Physiol. Rev. 78*, 921−947.
28. Guo, Y., Bozic, D., Malashkevich, V. N., Kammerer, R. A., Schulthess, T., and Engel J. (1998) *EMBO J. 17*, 5265−5272.
29. Efimov, V. P., Lustig, A., and Engel, J. (1994) *FEBS Lett. 341*, 54−58.
30. Vorherr, T., Wrzosek, A., Chiesi, M., and Carafoli, E. (1993) *Protein Sci. 2*, 339−347.
31. Ludlam, C. F., Arkin, I. T., Liu, X. M., Rothman, M. S., Rath, P., Aimoto, S., Smith, S. O., Engelman, D. M., and Rothschild, K. J. (1996) *Biophys. J. 70*, 1728−1736.
32. Karim, C. B., Stamm, J. D., Karim, J., Jones, L. R., and Thomas, D. D. (1998) *Biochemistry 37*, 12074−12081.
33. Kapust, R. B., and Waugh, D. S. (1999) *Protein Sci. 8*, 1668−1674.
34. Beck, K., Gambee, J. E., Kamawal, A., and Bächinger H. P. (1997) *EMBO J. 16*, 3767−3777.
35. O'Neil, K. T., and DeGrado, W. F. (1990) *Science 250*, 646−651.
36. Spek, E. J., Bui, A. H., Lu, M., and Kallenbach, N. R. (1998) *Protein Sci. 7*, 2431−2437.
37. Woolfson, D. N., and Alber, T. (1995) *Protein Sci. 4*, 1596−1607.
38. Pollesello, P., Annila, A., and Ovaska, M. (1999) *Biophys. J. 76*, 1784−1795.

BI0000972